ChemCatChem
Review
doi.org/10.1002/cctc.202201583
Chemistry Europe
European Chemical Societies Publishing
www.chemcatchem.org

Special Collection

In situ Reaction Monitoring in Photocatalytic Organic Synthesis

Amiera Madani[a, b] and Bartholomäus Pieber*[a]

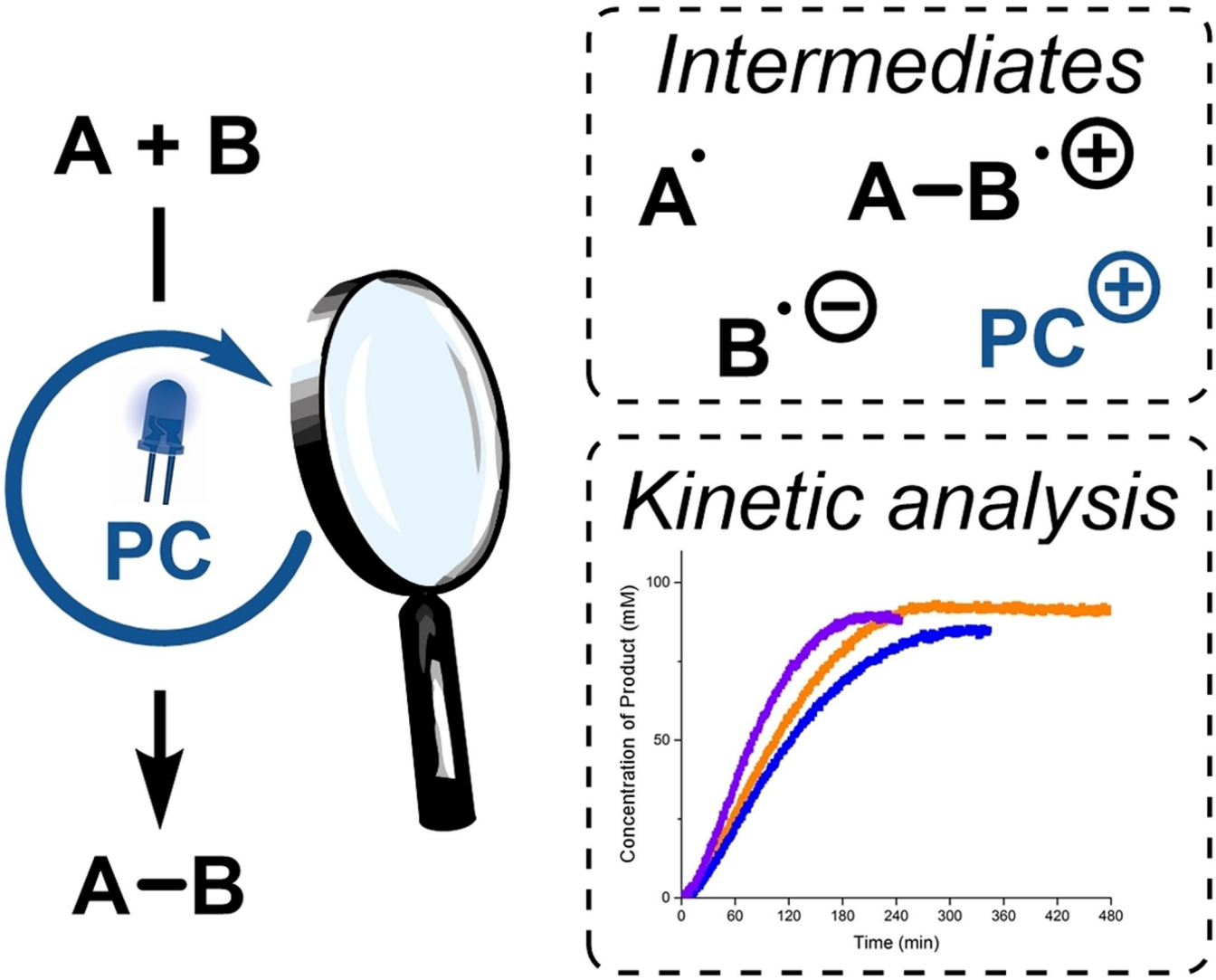

© 2023 The Authors. ChemCatChem published by Wiley-VCH GmbH

Visible-light photocatalysis provides numerous useful methodologies for synthetic organic chemistry. However, the mechanisms of these reactions are often not fully understood. Common mechanistic experiments mainly aim to characterize excited state properties of photocatalysts and their interaction with other species. Recently, in situ reaction monitoring using dedicated techniques was shown to be well-suited for the identification of intermediates and to obtain kinetic insights, thereby providing more holistic pictures of the reactions of interest. This minireview surveys these technologies and discusses selected examples where reaction monitoring was used to elucidate the mechanism of photocatalytic reactions.

1. Introduction

Visible-light photocatalysis has become a cornerstone of modern organic synthesis.[1] Key to success is the ability of certain chromophores, including organometallic complexes,[2] organic dyes[3] and semiconducting materials[4] to reach long-lived excited states that can act as single electron oxidants/reductants (photoredox catalysis, PRC),[5] transfer energy to substrates or reagents (energy transfer catalysis, EnT),[6] or serve as hydrogen atom transfer catalysts (HAT).[7] These events provide straightforward access to reactive open-shell intermediates under mild conditions and resulted in the development of a myriad of new reaction methodologies.[1]

Unraveling the mechanisms of these transformations is challenging, because many state-of-the-art photocatalytic transformations include more than one catalytic species and several reagents that are necessary to complete catalytic cycles.[1] Further, certain photocatalysts can act as SET, HAT and EnT catalysts, undergo consecutive photoinduced electron transfer events,[8] or access different reactivity depending on the photon energy/intensity leading to complex mechanistic scenarios.[9] It is therefore not surprising that more than one mechanism can be used to plausibly explain the outcome of photocatalytic transformations. Indeed, proposed mechanisms are critically discussed,[10] and were revised after careful investigations.[11]

The vast majority of mechanistic studies of photocatalytic reactions rely on experiments that aim to characterize the excited state properties of photocatalysts and their interaction with substrates, reagents and co-catalysts under idealized conditions.[12] These include computational and electrochemical methods, static optical spectroscopy, quantum yield analysis, quenching experiments, (ultra)fast spectroscopy and the identification of radical intermediates using trapping agents and radical clock experiments, as well as electron paramagnetic resonance (EPR) spectroscopy.[12] These experiments undoubtedly provide essential insights that build the foundation for mechanistic proposals.

However, more holistic pictures of photocatalytic reactions are highly desirable and require the determination of rate laws and studies on (thermal) follow-up events that typically occur on a comparably longer time scale than the initial photocatalytic activation steps. As such, real-time monitoring of reactions is a complementary analysis method that allows obtaining quantitative reaction profiles and identifying relevant species in solution, including catalysts, substrates, reagents, intermediates, products, as well as side- and byproducts.[13] The obtained profiles can be further processed using, for example, reaction kinetic progress analysis (RKPA) or variable time normalization analysis (VTNA) to extract valuable kinetic information.[13] Further, reaction monitoring provides important data to design and operate large scale reactions in a safe, controllable and reproducible manner.[14]

Although common for thermal reactions, real-time reaction monitoring has been only sparingly applied in synthetic photocatalysis, which likely results from the (slightly) higher complexity of setups capable of such analysis. Moreover, kinetic data of photochemical reactions is somewhat difficult to reproduce due to the strong dependence on the exact photochemical setup.[15] The spectral output (wavelength distribution, photon equivalents, etc.) of the light source and other factors, such as the distance between the light source and the reaction vessel, the reaction vessel itself (i.e. material and thickness), or temperature effects can directly impact reaction profiles.[15]

This minireview surveys in situ reaction monitoring approaches for photocatalytic reactions. The first part aims to provide a general overview over techniques that are used by synthetic organic chemists to monitor reaction profiles and intermediates in real-time. The second part discusses selected examples from the scientific literature, where these monitoring techniques shed light on the mechanism of photocatalytic reactions.

2. Techniques for reaction monitoring in photocatalysis

An ideal technique for reaction monitoring of photocatalytic reactions should provide information of all relevant species within a reaction mixture under synthetically relevant conditions with high sensitivity and sufficient temporal resolution. In

[a] A. Madani, Dr. B. Pieber
Department of Biomolecular Systems
Max-Planck-Institute of Colloids and Interfaces
Am Mühlenberg 1
14476 Potsdam (Germany)
E-mail: bartholomaeus.pieber@mpikg.mpg.de
Homepage: Homepage: https://www.pieberlab.com
[b] A. Madani
Department of Chemistry and Biochemistry
Freie Universität Berlin
Arnimallee 22
14195 Berlin (Germany)

Special Collection This publication is part of a Special Collection on "Photocatalytic Synthesis". Please check the ChemCatChem homepage for more articles in the collection.

© 2023 The Authors. ChemCatChem published by Wiley-VCH GmbH. This is an open access article under the terms of the Creative Commons Attribution License, which permits use, distribution and reproduction in any medium, provided the original work is properly cited.

practice, no technology that fulfills all requirements for the broad range of photocatalytic methods is available to date. The practitioner has to choose between different approaches on a case-by-case basis depending on the specific needs of the reaction of interest.

In addition to design criteria that are specific to light-mediated reactions (light source, vessel materials, etc.), other factors have to be taken into consideration. For example, many homogeneous solution-phase reactions can be carried out reliably in a nuclear magnetic resonance (NMR) spectrometer,[16] whereas heterogeneous (solid-liquid, gas-liquid, gas-liquid-solid) transformations typically require other techniques due to problems associated with mixing. Moreover, paramagnetic species complicate NMR measurements and data interpretation, specifically for quantitative analysis.[17]

In general, all nondestructive analytical methods, including NMR spectroscopy and vibrational spectroscopy (FTIR, Raman) are suitable for reaction monitoring. Depending on the technique, the reaction has to be carried out inside of the analytical instrument or by using a dedicated probe that can be inserted into a reaction vessel. Alternatively, destructive methods, such as mass spectrometry (MS), that continuously analyze small aliquots of the reaction mixture in an automated fashion, without significantly altering its chemical composition and scale, can be used.[18] However, quantification is limited and MS techniques are typically not used for monitoring the concentration of specific species over time. Nevertheless, MS analysis is ideally suited for the identification of (reactive) intermediates, which can be important for elucidating reaction mechanisms. As such, we have included relevant technologies and examples in this minireview.

2.1. NMR spectroscopy

NMR spectroscopy is a non-destructive and non-invasive technique that is routinely used in synthetic organic chemistry for the identification and quantification of products, substrates, reagents as well asintermediates .[19] A particular strength is the complementary structural information of dissolved molecules that can be gained by multi-nuclear detection (^{1}H, ^{13}C, ^{19}F, ^{31}P, ^{11}B, etc.) and two-dimensional NMR techniques (DOSY, NOESY, HSQC, HMBC, etc.). Reaction monitoring using in situ NMR measurements is also commonly applied to obtain kinetic insights.[13] Illuminating solutions inside NMR spectrometers mainly relies on setups that use waveguides to transport photons from the respective light source into the NMR vial.[20] The most common approach used for real-time monitoring of photocatalytic reactions is the fiber optic LED-NMR illumination setup that was developed by Gschwind and co-workers.[20c] Here, light from a high power LED is guided into the sample by an optical fiber. Uniform irradiation is achieved by roughening the fiber tip that is immersed into the reaction mixture through a coaxial insert (Figure 1, A). Fiber optic LED-NMR was also combined with optical spectroscopy to simultaneously acquire UV/Vis and NMR spectra.[21]

A related illumination setup uses the NMR tube itself as waveguide (Figure 1, B).[22] Here, the LED is positioned directly at the top of the NMR tube rather than outside of the spectrometer. Good sample illumination is achieved through abrasive etching of the exterior surface of NMR tubes in the sample area.

Although powerful, these waveguide-based setups use a single LED and therefore only provide relatively low light intensities. Roughening of the fiber tip as well as the abrasive etching of the NMR tube might cause reproducibility problems. Furthermore, these approaches do not enable the use of pressurized NMR tubes. A recently developed LED irradiation insert for NMR probes overcomes these problems (Figure 1, C).[23]

It is, however, important to note that reaction monitoring using NMR is limited to homogeneous reactions, because heterogeneous reaction mixtures require vigorous stirring to achieve reproducible and synthetically relevant results. Solid

Amiera Madani completed her undergraduate studies in chemistry at the University of Tübingen (Germany). In 2019 she joined the Max-Planck-Institute of Colloids and Interfaces in Potsdam (Germany) as a PhD student. Her research focuses on the development and mechanistic investigation of reactions involving reactive open-shell intermediates.

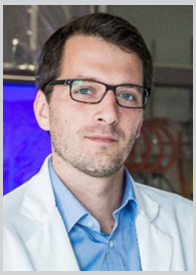

Bartholomäus (Bart) Pieber studied chemistry at the University of Graz (Austria), where he completed his PhD in the group of C. Oliver Kappe in 2015. Following his doctoral work, Bart moved to Peter Seeberger's lab in Potsdam (Germany). In 2018, he started his independent research career as a group leader at the Max Planck Institute of Colloids and Interfaces (Potsdam, Germany) and was appointed as a lecturer at the University of Potsdam. In 2022, he spent time as visiting scholar at the California Institute of Technology (Pasadena, USA, Host: Prof. Greg Fu). In summer 2023, his team will move to the Institute of Science and Technology Austria (ISTA), where he is joining faculty as an Assistant Professor (tenure track). The research of his team focuses on catalytic methods for organic synthesis using visible-light as energy source.

© 2023 The Authors. ChemCatChem published by Wiley-VCH GmbH

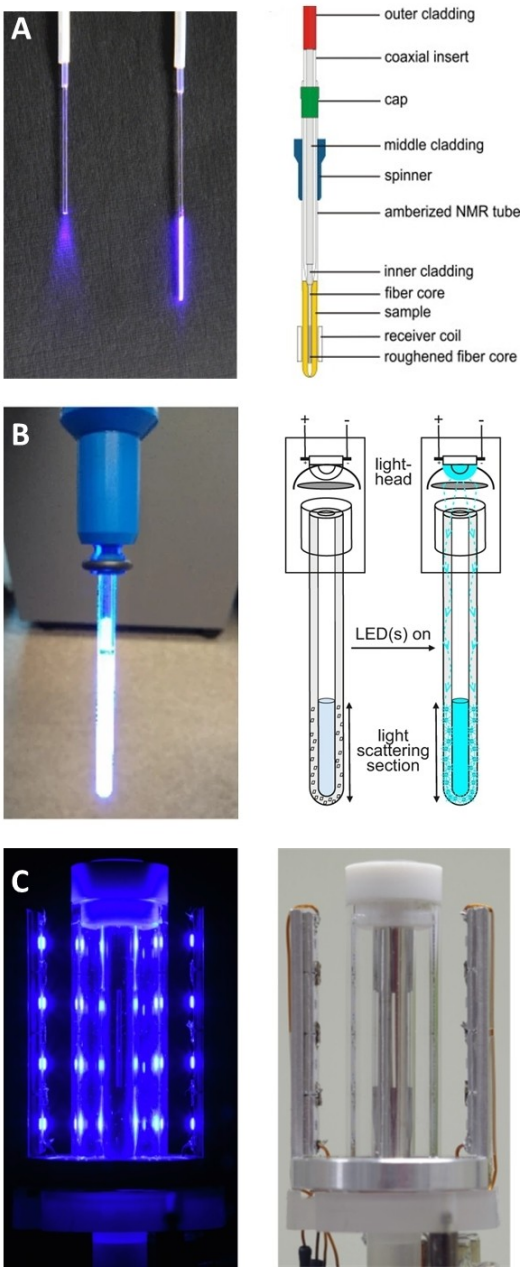

Figure 1. LED-NMR setups for in situ reaction monitoring of photochemical reactions. Irradiation is realized using a fiber optic (A) and the NMR tube itself as waveguide (B), or using a LED insert for NMR probes (C). Reproduced from ref. [20c], [22] and [23] with permission from Elsevier and Springer Nature.

catalysts or reagents settle without proper mixing, which has detrimental effects on the quality of the data obtained. In special cases, depositing heterogeneous photocatalysts on the inner wall of NMR tubes might be an option to address this limitation.[24]

2.2. Vibrational and optical spectroscopy

In contrast to NMR analysis, real-time vibrational and optical spectroscopy can be carried out using dedicated probes rather than immersing the reaction vessel into an analytical device.[25] These methods are not limited to homogeneous reactions and small scales. Fourier-transform infrared spectroscopy (FTIR) is among the most convenient and simultaneously broadly applicable methods for monitoring organic transformations.[26] It provides a molecular fingerprint of the chemical composition of compounds in solution and the change of signal intensity of a functional group of substrates or products can be related to their concentration. Attenuated total reflectance (ATR) is the most widely used technology for devices that enable static and time-correlated FTIR studies. In brief, this technique is based on multiple reflection of an IR beam within a crystal (i.e. silicon, or diamond) that is in contact with the sample. The interaction of the beam with the sample leads to detectable changes that can be processed to result in a typical infrared spectrum. ATR enabled the design of commercially available probes that can be directly dipped into a reaction vessel to continuously record FTIR spectra of (photocatalytic) transformations (Figure 2).[25a] The same technology is used for UV/Vis and fluorescence probes. However, the absorption and emission of photocatalysts dominates UV/Vis and fluorescence spectroscopy spectra, limiting the applicability of these techniques for reaction monitoring of photocatalytic reactions.[25e]

Raman spectroscopy allows to monitor gases, substances in solution and undissolved particles using fiber optic probes and is therefore broadly applicable in chemical analysis.[25b–d] Raman probes are either immersed into the reaction mixture (invasive), or placed outside of a transparent reaction vessel (non-invasive).[25f] In general, invasive probes, including the ATR-FTIR

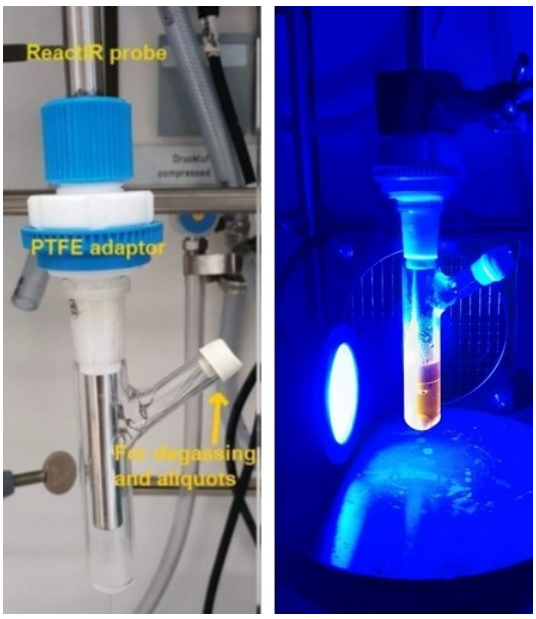

Figure 2. Setup for in situ reaction monitoring of photocatalytic reactions using an ATR-FTIR probe.

© 2023 The Authors. ChemCatChem published by Wiley-VCH GmbH

and FTIR-UV/Vis devices described above, impact the irradiation characteristics (smaller path length, reflection phenomena, etc.). This can lead to different time-profiles compared to a reaction carried out without a probe. Thus, non-invasive Raman probes are advantageous, because reaction monitoring can be carried out using completely unaltered setups. Another advantage of Raman spectroscopy over other techniques is that signals do not typically interfere with water vibrational modes, allowing its use in aqueous reactions.[25f] However, for photocatalytic applications the light source and the fluorescence of a chromophore may interfere, resulting in a lowering of the signal-to-noise ratio, which limits its application in photochemistry.[25e]

2.3. Mass spectrometry

The high sensitivity of modern mass spectrometry instruments allows to detect species that are present in very low concentrations in reaction mixtures.[27] More importantly, MS allows to identify reactive intermediates that are otherwise only (indirectly) accessible using trapping and radical clock experiments.[12] This can result in mechanistic hints that are hard to obtain using other techniques. However, analyzing (photo)chemical reactions via mass spectrometry in a batch setup requires an interface that constantly delivers small aliquots of the reaction mixture to a mass spectrometer (ex situ). A prototype setup using a probe electrospray ionization mass spectrometer (PESI-MS) was recently developed for such purposes (Figure 3).[28] This technology is based on a stainless steel acupuncture needle that repeatedly transfers small aliquots of the reaction mixture directly to the ion source with an estimated time of 575 ms per sampling cycle. The reactor consists of a stirred reaction vessel with a sampling orifice and a light source. Importantly, the probe surface conditions were reported to play a key role in the signal consecutiveness in PESI-MS experiments. An untreated acupuncture needle gave inconsistent results, which was attributed to the attachment of photocatalyst particles (TiO_2) on the probe tip. Surface modification of the tip with TiO_2 eliminated these problems.

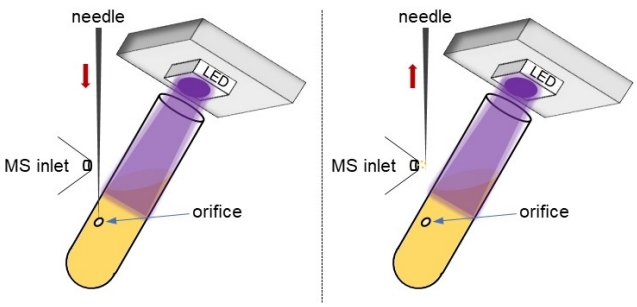

Figure 3. Monitoring photocatalytic reactions using PESI-MS.

2.4. Reaction monitoring using flow techniques

In continuous flow chemistry, non-destructive analytical methods that enable real-time analysis are directly integrated after a (photo)reactor unit via an analytical flow-through cell (termed in-line analysis). Common techniques include FTIR,[29] Raman,[30] UV/Vis,[31] or (benchtop) NMR spectroscopy[32] and are nowadays regularly applied due to their "plug-and-play" nature (Figure 4, A). Reaction monitoring at preparative scales using destructive analytical methods, such as mass spectrometry, requires setups that periodically sample aliquots or split the flow stream (termed on-line analysis) (Figure 4, B).[33] Analysis of flow chemical reactions using such process analytical techniques is fundamentally different to reaction monitoring in batch reactions for two reasons. First, batch reactions require monitoring techniques that analyze a chemical transformation directly in (or sample continuously from) the reaction vessel, whereas monitoring of flow reactions is spatially decoupled from the reactor unit.[34] Second, in batch the substrate concentration is uniformly distributed throughout the flask and decreases exponentially over time. In a flow reaction, the concentration of the starting material decreases along the reactor unit reaching a minimum at its end. Consequently, monitoring a flow reaction under steady state conditions gives continuous feedback of a reaction at a fixed reaction time, which is, for example, used to evaluate the stability of heterogeneous photocatalysts in packed-bed reactors.[35] Tracking the time course in flow, on the contrary, requires a multitude of experiments with varied flow rates under steady state conditions[36] and is therefore not discussed in this minireview.

More relevant approaches in the context of this minireview are flow techniques that directly feed a reaction mixture into a mass spectrometer and irradiate the catalytic cocktail either before, or only at the tip of an ESI-MS spray capillary (Figure 5).[37] This approach (termed "photoflow ESI-MS" throughout this minireview) allows to identify (short-lived) reactive intermediates that are generated during photochemical processes and can therefore give important mechanistic insights. For

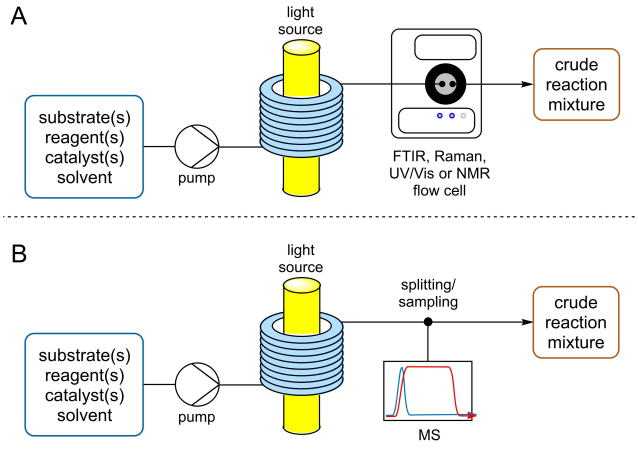

Figure 4. Reaction monitoring in flow photocatalysis. Nondestructive analytical tools are directly integrated in the flow path (A), whereas destructive methods require splitting or sampling techniques (B).

© 2023 The Authors. ChemCatChem published by Wiley-VCH GmbH

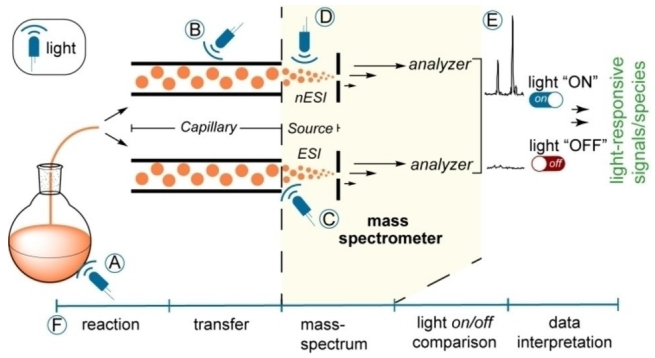

Figure 5. Monitoring (short-lived) intermediates in photocatalysis by directly feeding the reaction mixture into an ESI-MS device (photoflow ESI-MS). Irradiation can be carried out in the flask or syringe (A), in the capillary (B); on the tip of the capillary and plume at the needle tip (C), or on the tip of a nanospray-ESI (nESI) device (D). Reproduced from ref. [37e] with permission from John Wiley and Sons.

detailed discussions on these techniques, we refer to specialized, we refer to specialized reviews by the groups of Ananikov[37e] and Roithovà.[37d]

3. Mechanistic insights gained through reaction monitoring

3.1. Identification of intermediates

The flavin catalyzed photooxidation of 4-methoxybenzyl alcohol (MBA) was among the first photocatalytic reactions that was studied using a fiber optic LED-NMR setup (Figure 6, A).[38] Reaction monitoring under anaerobic conditions was carried out in combination with chemically induced dynamic nuclear polarization (CIDNP) experiments, which allow the detection of short-lived radical species.[39] These studies provided evidence that different mechanisms are operating depending on the reaction medium. A slow reaction that likely proceeds via a formal two-electron-transfer mechanism on the NMR timescale was observed in CD_3CN. The same reaction proceeded significantly faster in a CD_3CN:D_2O mixture. More importantly, line broadening of the NMR signals under aqueous conditions was indicative for a long-lived semiquinone radical species ($RFTA^{\cdot+}$, confirmed by UV/VIS spectroscopy), suggesting a single-electron transfer mechanism. The authors concluded that this results from the stabilization and separation of the radical counterions in presence of D_2O, whereas non-aqueous conditions lead to contact ion pairs that facilitate back electron transfer.

Another oxidative flavin catalyzed reaction was investigated using photoflow ESI-MS monitoring (Figure 6, B).[40] More specifically, the authors studied the aerobic oxidation of toluene derivatives using a chiral ethylene-bridged flavinium salt that leads to the corresponding benzyl alcohols and benzaldehydes. Various reaction times were simulated by irradiating the reaction mixture in a flow reactor before entering the mass

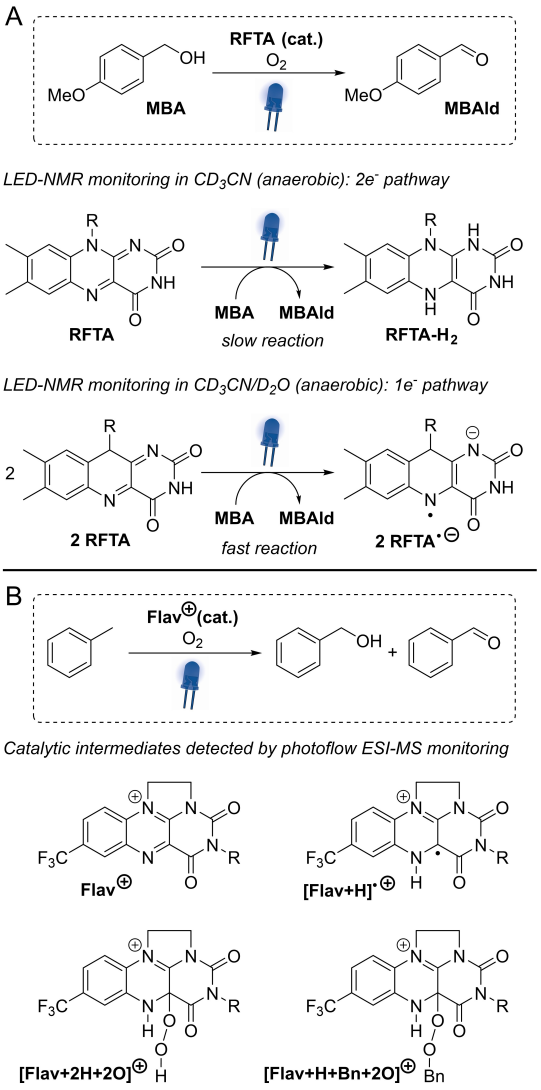

Figure 6. Reaction monitoring in flavin photocatalysis. LED-NMR studies revealed that the solvent impacts the reaction mechanism (A). Photoflow ESI-MS monitoring provided evidence for several catalytic intermediates (B).

spectrometer, or only at the tip of the spray capillary. Several short-lived species were identified that agree with postulated intermediates of a plausible catalytic cycle. In addition, a series of side-products, including arylated flavinium ions, were detected and attributed to result from undesired off-cycle events. It is worth noting that all detected intermediates were further confirmed by isotope labelling studies, as well as IR and UV/Vis spectroscopy.

Tetrahydroisoquinolines (THIQs) are amongst the most studied substrates that are activated through photoredox catalysis. These reactions are typically proposed to involve the initial formation of the corresponding radical cation via single electron oxidation that opens opportunities for several follow-up reactions.[41] A classic example is the photocatalyzed aza-Henry reaction of THIQs and $MeNO_2$ that was originally reported by the Stephenson laboratory.[42] The groups of König and Gschwind reported an extensive mechanistic study of this

© 2023 The Authors. ChemCatChem published by Wiley-VCH GmbH

transformation that included reaction monitoring using a fiber optic LED-NMR setup under anaerobic conditions.[43] In addition to the substrate (**1**) and product (**2**), the authors were able to identify and monitor the formation and consumption of a dimeric species (**3**) and nitrone **4** (Figure 7). Further, iminium ion (**5**) as well as THIQ-OOH (**6**) that results from reaction with residual oxygen were identified in low concentrations during the initial phase of the reaction. Additional experiments under aerobic conditions were carried out by analyzing aliquots of a batch reaction via ex situ NMR. Here, a significantly faster reaction rate was observed and THIQ-OOH (**6**) was identified as main intermediate. Based on these observations, the authors carefully studied the formation and fate of these species. These investigations resulted in a complex mechanistic picture of the photocatalytic aza-Henry reaction that consists of several pathways that lead to the formation of the desired product. In brief, photocatalytic initiation generates the key radical cation that leads to the desired product under aerobic conditions via **5**, or a α-amino radical. The α-amino radical was also proposed to trigger formation of dimer **3** and nitrone **4** under anaerobic conditions via two different pathways. Both species are converted to the desired product. The authors also provided evidence for two productive background reactions that do not involve the photocatalyst.

Photoredox catalysis can be used to convert 1,2,3,4-tetrahydroquinoline into quinoline under aerobic conditions (Figure 8, A).[37c] This reaction was discovered using a photoflow ESI-MS approach as reaction screening tool that also identified a radical cation intermediate and the reduced photocatalyst ($Ru(bpy)_3^+$). Similar intermediates were detected during a photoflow ESI-MS study of the photocatalytic [3 + 2] annulation of N-cyclopropyl aniline and styrene (Figure 8, B).[44]

The groups of Ananikov and König developed a photoredox catalyzed Markovnikov-type thiol-yne reaction of terminal alkynes and thiophenol derivatives.[45] To support their mechanistic rationale, an alkyne with an ionizable sulfate group (**7**) was synthesized to study the formation of the desired product (**8**) and an undesired side product (**9**) via photoflow ESI-MS reaction monitoring (Figure 9, A). More recently, the same groups extended this photocatalytic method to an intermolecular thiol-yne-ene reaction.[46] The reaction was studied using alkyne **7**, 2-fluorothiophenol (**10**) and vinylsulfide **11** in presence of (tert-butyl)-N-(perfluorobiphenyl-4-yl)oxylamine (**12**) as radical trap with a high resolution photoflow ESI-UHRMS monitoring setup (Figure 9, B). In presence of green light, radical adduct **13** was detected, indicating that **14** is a reactive intermediate.

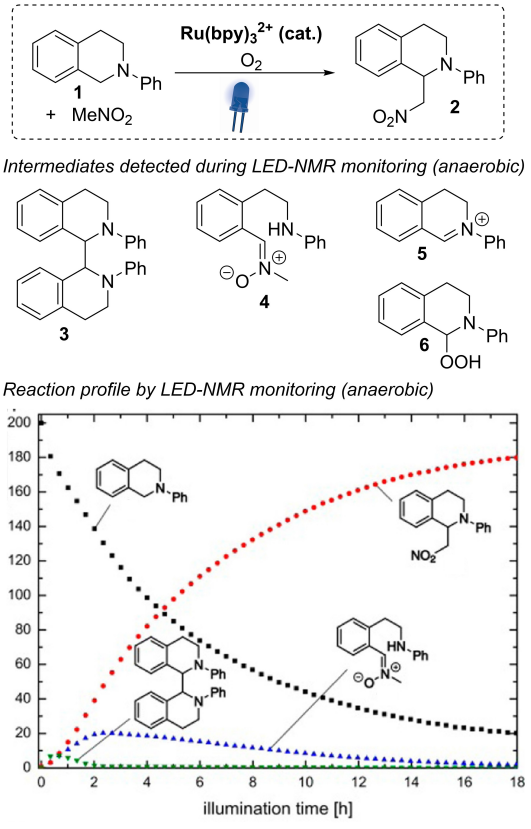

Figure 7. Monitoring of the photocatalytic aza-Henry reaction by LED-NMR identified several productive intermediates. Reproduced from ref. [43] with permission from the American Chemical Society.

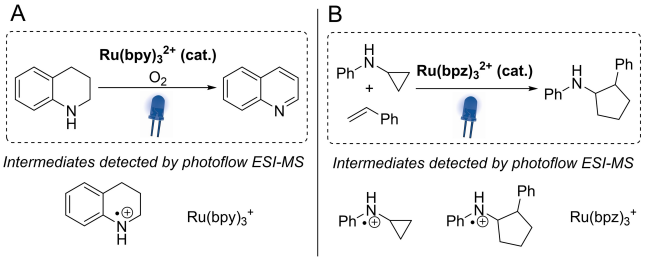

Figure 8. ESI-MS monitoring of photocatalytic reactions of amines identified radical cation intermediates and reduced photocatalyst species.

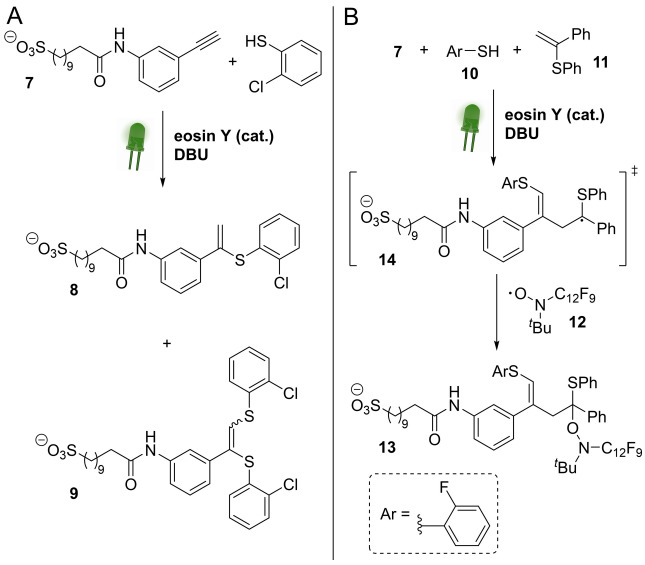

Figure 9. Photoflow ESI-(UHR)MS reaction monitoring of a photocatalytic thiol-yne (A) and a thiol-yne-ene reaction (B).

© 2023 The Authors. ChemCatChem published by Wiley-VCH GmbH

Photoflow ESI-MS monitoring was also applied to identify intermediates in the photocatalytic Meerwein arylation of pyrazin-2-amine with 4-methoxybenzenediazonium tetrafluoroborate (Figure 10, A).[47] This study provided evidence that the reaction proceeds through the formation of radical cation **15.**

Schultz and coworkers used decatungstate photocatalysis for the oxygenation of amines in presence of hydrogen peroxide under acidic conditions.[48] Using LED-NMR and photoflow ESI-MS monitoring, **16** was identified as key intermediate when pyrrolidine was used as substrate (Figure 10, B). This observation suggested that oxygen might also serve as a suitable oxidant and the authors subsequently showed that an aerobic oxidation is indeed feasible.

Reaction monitoring further gave key insights in the photocatalytic C(sp^3)-F bond cleavage of trifluoromethylarenes to produce aryldifluoromethyl compounds using stoichiometric amounts of pinacolborane (HBpin) and 2,2,6,6-tetramethylpiperidine (TMP). (Figure 10, C).[49] Using a LED-NMR setup the authors tracked the reaction via ^{11}B-NMR and observed the formation of borenium cation **17**. Subsequent mechanistic experiments indicated that this Lewis acidic species, which is formed in situ from protonated TMP and HBpin, plays an important role in the key C–F bond abstraction.

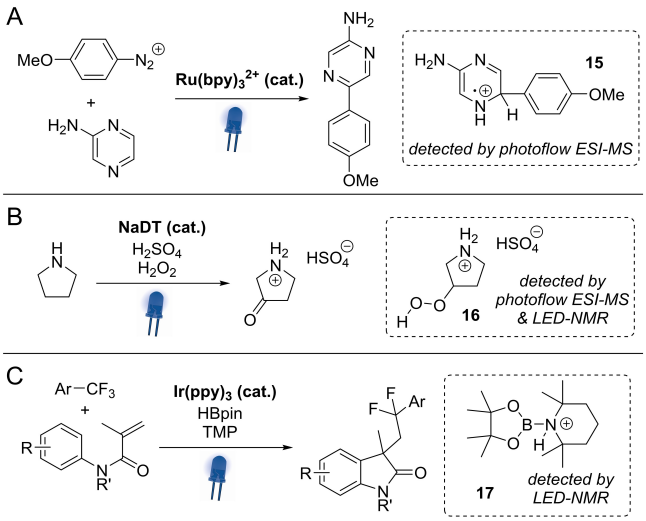

Figure 10. Intermediates identified through reaction monitoring of the photocatalytic Meerwein arylation (A) the photocatalytic oxygenation of amines (B), and the photocatalytic C(sp^3)-F bond cleavage of trifluoromethylarenes (C).

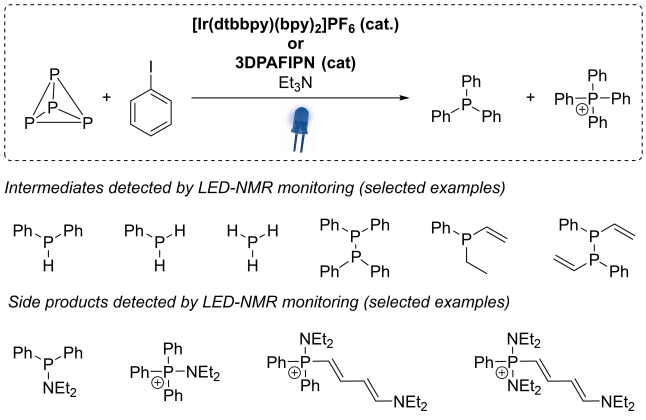

Figure 11. Intermediates and side products in the photocatalytic arylation of white phosphorous identified through reaction monitoring using LED-NMR.

In a collaborative effort, the groups of Gschwind and Wolf showed that [Ir(dtbbpy)(bpy)$_2$]PF$_6$ can trigger the reaction of white phosphorous (P_4) and aryl iodides to yield valuable triarylphosphines and tetraarylphosphonium salts in presence of blue light and triethylamine as sacrificial electron donor.[50] Time resolved ^{31}P-NMR analysis of the reaction between P_4 and iodobenzene using a LED-NMR setup was used to track the reaction. These experiments visualized the evolution and consumption of primary, secondary and tertiary monophosphine intermediates, and identified traces of Ph_4P_2, benzene and Et_2NH as minor side-products (Figure 11). A follow-up study using an organic photocatalyst (3DAFIPN) revealed numerous additional intermediates and side-products that are derived from a non-innocent behavior of Et_3N.[51] Of specific interest was the identification of PH_3, which prompted the authors to develop an alternative strategy that can directly convert this industrial P_1 precursor to several Ar_3P and Ar_4P^+ products using a similar photocatalytic protocol.

3.2. Kinetic analysis

Reaction monitoring enables detailed kinetic analysis to gain a holistic understanding of chemical reactions under native reaction conditions. In the case of photocatalytic reactions, care has to be taken, as kinetic studies may give data obfuscated by turnover-limiting processes derived from interaction between the excited photocatalyst and the respective quencher. In other words, the practitioner has to keep in mind that, depending on the conditions, the reaction of interest may be "photon-limited" or "photon-unlimited". Under photon-limited conditions, reaction rates depend on the absorption of photons and are typically zero-order in the photocatalyst. Photon-unlimited regimes refer to a situation where the quencher is constantly saturated with excited photocatalyst species. Under such conditions, the excited photocatalyst can be essentially treated as a reagent in high excess.

Yoon and colleagues studied the kinetics of an enantioselective intramolecular [2+2] cycloaddition that is catalyzed by a chiral iridium photocatalyst (Figure 12).[52] The authors initially monitored the concentration of substrate and product over time using an LED-NMR setup, which showed that the reaction is complete within less than three minutes. Initial rate studies by several LED-NMR experiments showed a first order dependency in photocatalyst concentration and light intensity (Figure 12) as well as zero-order in substrate. Consequently, the authors concluded that the model reaction operates in a photon-unlimited regime under these monitoring conditions.

More recently, the same group reported a detailed kinetic analysis of a related intermolecular [2+2] cycloaddition using the same chiral photocatalyst.[53] Visual kinetic analysis techni-

© 2023 The Authors. ChemCatChem published by Wiley-VCH GmbH

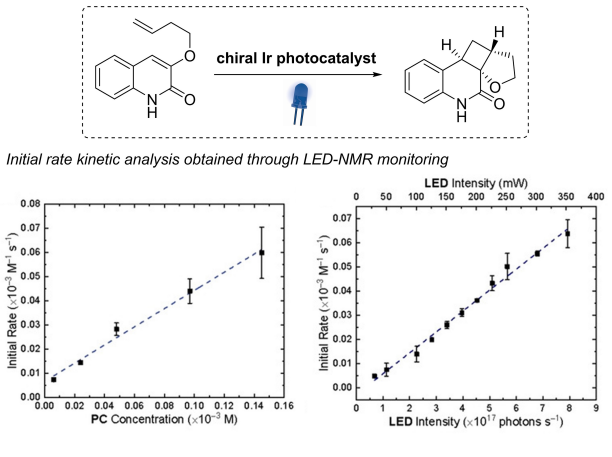

Figure 12. Initial rate kinetic analysis using LED-NMR of an enantioselective photocatalytic intramolecular [2+2] cycloaddition. Reproduced from ref. [52] with permission from John Wiley and Sons.

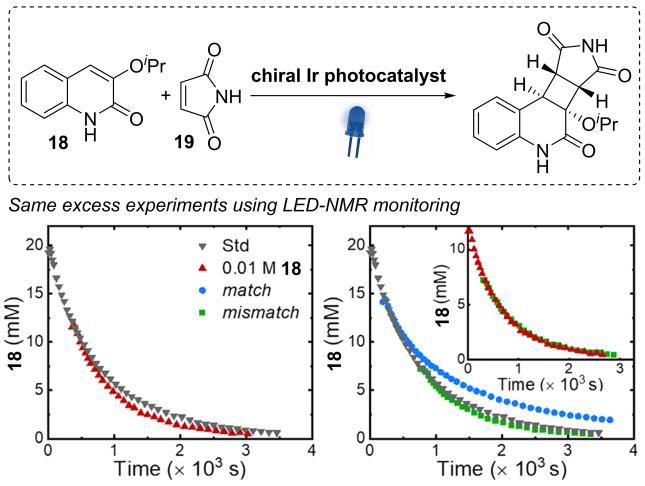

Figure 13. Same excess experiments of a photocatalytic intermolecular [2+2] cycloaddition. Left: Same excess comparison between standard condition and conditions that mimic 40% conversion. Right: Comparison of standard conditions to conditions approximating 30–50% conversion with the addition of the expected concentration of the product. Blue = matched Ir and product chirality; green = mismatched Ir and product chirality. Reproduced from ref. [53] with permission from the American Chemical Society.

ques using data obtained from LED-NMR monitoring experiments were used to extract kinetic information. A "same excess" experiment was carried out. Here, the initial concentration of starting materials for two reactions using LED-NMR monitoring was different, but chosen in a way that the experiments allow comparison of sections of the reaction profiles that have same concentration of reactants, but different concentration of product. These experiments mimic different turnovers of the catalyst to determine if the reaction suffers from product inhibition or catalyst deactivation. Non-overlaying reaction profiles are indicative for product inhibition or catalyst deactivation and require further experiments for clarification. The same excess experiment of the [2+2] cycloaddition of **18** and maleimide indeed showed that the profiles do not overlay (Figure 13, bottom left). The authors carried out additional experiments in presence of the enantioenriched product and the matched and mismatched chiral photocatalyst, which provided evidence that product inhibition by the major enantiomer is responsible for the outcome of the same excess experiment (Figure 13, bottom right).

Next, rate laws for the title reaction at different temperatures were constructed from reaction profiles using variable time normalization analysis (VTNA).[53] Therefore, multiple reaction profiles are collected by strategically changing the concentration of a single ingredient of the reaction mixture ("different excess" experiments). Normalizing the time between each pair of data points using the VTNA approach enables to determine the order in each parameter through a graphical overlay comparison. Therefore, the time-scale is substituted by the time integral of the reagent concentration, taken to an arbitrary power α [Eq. (1)]. The value for α that leads to an overlay of the graphs, is the order of the respective reagent.

$$\int_{t=0}^{t=n} [A]^{\alpha} dt = \sum_{i=1}^{n} \left(\frac{[A]_i - [A]_{i-1}}{2} \right)^{\alpha} (t_i - t_{i-1}) \quad (1)$$

Interestingly, VTNA of the cycloaddition resulted in different rate laws at different temperatures (Figure 14). Under both conditions the rate is first-order in light intensity and zero-order in photocatalyst concentration, which is indicative of a photon-limited regime. The dependency on the substrates, on the contrary, changes depending on the temperature. This suggests that the mechanism of asymmetric product formation varies as a function of temperature. The rate law obtained under cryogenic conditions agrees with a bimolecular energy transfer mechanism that was previously postulated based on DFT calculations,[54] whereas the rate law at room temperature is more indicative for an intramolecular energy transfer mechanism.

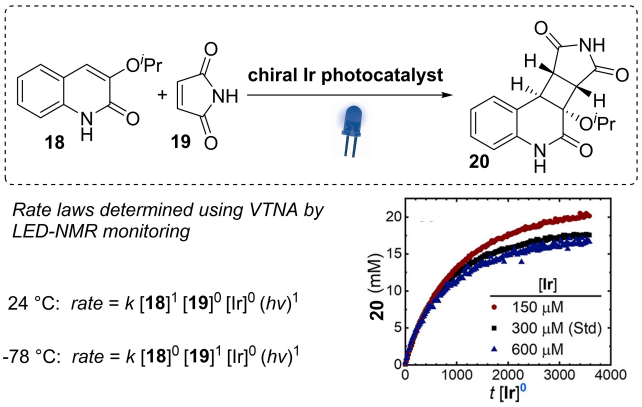

Figure 14. Rate laws of a photocatalytic intermolecular [2+2] cycloaddition determined at different temperatures using LED-NMR monitoring and VTNA. Bottom right: VTNA overlay for [Ir] at 24 °C. Reproduced from ref. [53] with permission from the American Chemical Society.

© 2023 The Authors. ChemCatChem published by Wiley-VCH GmbH

VTNA was also applied to study the metallaphotocatalytic C–O arylation of methyl 4-iodobenzoate (**21**) with N-Boc-proline (**22**) using a nickel catalyst in combination with either $Ir(ppy)_3$ or a graphitic carbon nitride (CN-OA-m) as photocatalyst (Figure 15).[25a] Due to the heterogeneous nature of CN-OA-m, an ATR-FTIR probe was the reaction monitoring tool of choice for this comparative study. The reaction was studied with both photocatalysts under photon-limited and photon-unlimited conditions. The photon-unlimited regime was postulated to be of specific interest, because under such conditions the photocatalyst drops out of the rate law enabling a direct comparison of both methods. Interestingly, the authors found that the kinetics of the two catalytic systems are not identical. In case of the carbon nitride catalyst, a fractional order of aryl iodide **21** was determined, indicating that the photocatalyst activates **21** before it enters the nickel catalytic cycle. The authors further found that the iridium photocatalyst is less selective under photon-unlimited conditions and identified a significant amount of the corresponding protodehalogenation side product. Moreover, same excess experiments indicated catalyst deactivation, which was later shown to be likely resulting from the formation of nickel-black.[55]

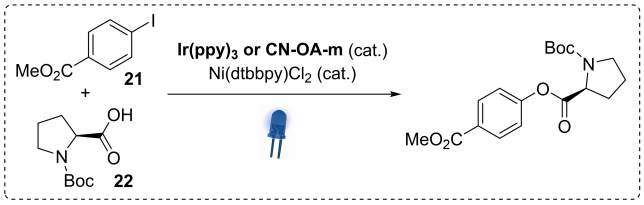

Rate laws determined using VTNA by ATR-FTIR monitoring

CN-OA-m	$Ir(ppy)_3$
Photon-unlimited: *rate* = *k* [**Ni**]^1 [**21**]$^{0.3}$	Photon-unlimited: *rate* = *k* [**Ni**]^1
Photon-limited: *rate* = *k* [**21**]$^{0.3}$	Photon-limited: *rate* = *k* [**Ni**]^1

Figure 15. Rate laws of a metallaphotocatalytic C–O arylation obtained using ATR-FTIR monitoring and VTNA using two different photocatalysts under photon-limited and photon-unlimited reaction regimes.

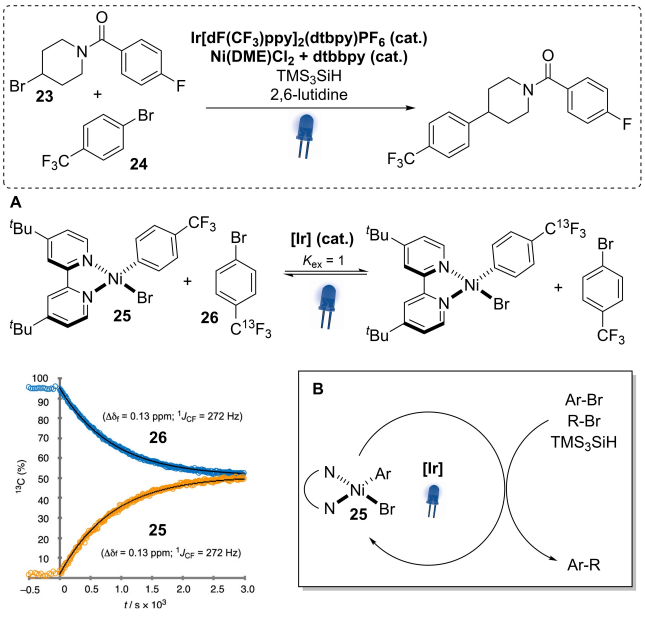

Figure 16. Metallaphotocatalytic cross-electrophile-coupling studied via LED-NMR reaction monitoring identified a photochemical exchange phenomenon (A). This provided evidence that intermediate **25** is responsible for product formation (B). Reproduced from ref. [56] with permission from the American Chemical Society.

A metallaphotocatalytic cross-electrophile-coupling of aryl bromide **23** and alkyl bromide **24** was investigated using online monitoring with a LED-NMR setup (Figure 16).[56] The initial reaction profile (^{19}F-NMR) showed not only the generation of the desired product, but also led to the identification of two minor side products arising from a coupling reaction of the aryl bromide with the solvent (Ar-solv) and protodehalogenation of **24** (Ar–H). More importantly, a transient Ni^{II} species (**25**) was identified. Isotope entrainment experiments using **25** in presence of **26**, the photocatalyst and light unveiled a hitherto unreported exchange phenomenon (Figure 16, A). Based on that finding, further investigations were carried out, which provided evidence for a mechanistic scenario in which product formation occurs directly through **25** (Figure 16, B).

With that finding in hand, the authors performed a detailed visual kinetic analysis that included alterations of all seven components of the catalytic cocktail (40 different sets of conditions). These investigations led to a series of important insights into this transformation under LED-NMR conditions. For example, the rate of the aryl bromide consumption was shown to be controlled by the concentration of the Ni catalyst, the photocatalyst, the photon flux and the aryl bromide (**23**). The rate of turnover approaches concentration independence (= saturation) in **23**. Excess of $(TMS)_3SiH$ and **24** are responsible for the high selectivity of this C–C coupling. Changes in catalyst loadings do not necessarily translate directly into changes in the rate of productive catalysis. Moreover, complex **25** and the photocatalyst compete for incident photons. With these data in hand, the authors constructed a minimal kinetic model for the title reaction (Figure 17, A). The flow diagram shows five discrete events that control the rate of product formation (fractionations f_1-f_5). A series of simulations using this model resulted in kinetic behavior that is reconciled with two plausible mechanisms, which only differ in the interaction between the photo- and the nickel catalyst (single electron transfer versus energy transfer) (Figure 17, B).

3.3. Miscellaneous

Reaction monitoring is not only a powerful tool to identify intermediates and gain kinetic information, but also allows to gain insights into other aspects of photocatalytic reactions. For example, a LED-NMR setup was used to visualize that tert-butyl nitrite (TBN) is key to realize the light-mediated cleavage of benzyl ether protective groups using 2,3-dichloro-5,6-dicyano-1,4-benzoquinone (DDQ) as photocatalyst (Figure 18, A).[57] In the absence of TBN, the reaction stopped after a single turnover of the photocatalyst. Delayed injection of excess TBN immedi-

© 2023 The Authors. ChemCatChem published by Wiley-VCH GmbH

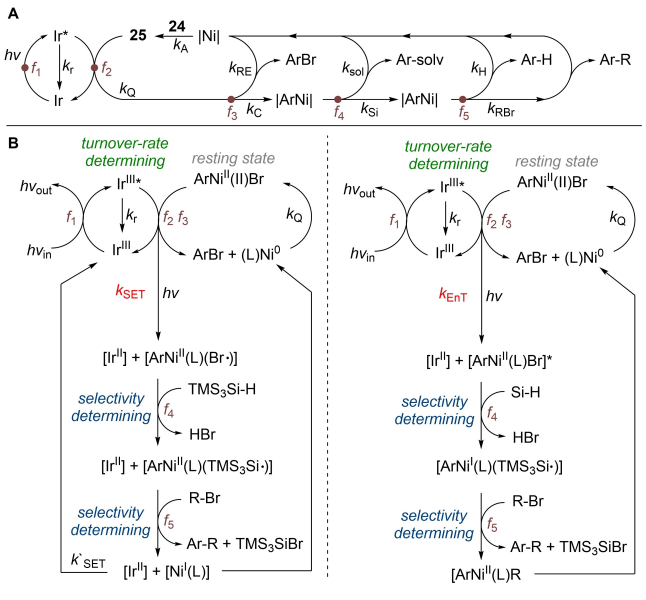

Figure 17. Minimal kinetic model for simulations of the metallaphotocatalytic cross-electrophile coupling (A). These simulations agree with two mechanistic proposals (B).

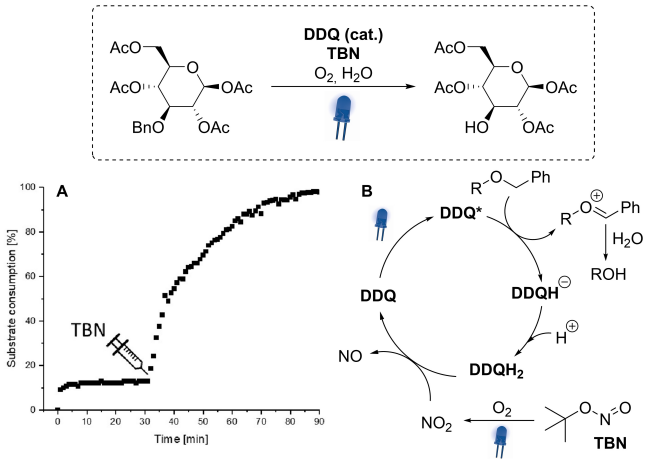

Figure 18. Reaction monitoring of a photocatalytic benzyl ether cleavage. Only one turnover of the photocatalyst is observed before addition of TBN (A), because TBN is required to close the catalytic cycle (B). Reproduced from ref. [57] with permission from the American Chemical Society.

ately started further product formation and the reaction proceeded until completion. This provides evidence that TBN photochemically releases NO, which is ultimately oxidized to NO_2 by dissolved O_2 (Figure 18, B). The potent gaseous oxidant converts 2,3-dichloro-5,6-dicyano-1,4-dihydroquinone ($DDQH_2$) to DDQ to close the catalytic cycle.

The authors further carried out a light on/off experiment using the LED-NMR setup that showed that no product is formed when the light source is switched off. Such experiments are carried out to study if chain processes are active or not. However, care has to be taken when conclusions are drawn from such experiments, because no product formation in the absence of light does not conclusively rule out radical chain involvement.[58]

Nevertheless, light on/off experiments can lead to important discoveries. An interesting example was reported by Lenherr, Ji and coworkers during their development of a cycloisomerization of alkynols using an iron pre-catalyst that is activated using visible-light (Figure 19).[59] In addition to qualitative observations that showed an induction period, initial rate studies to identify the photon-limited and unlimited regime, same-excess experiments that indicated catalyst deactivation and reaction progress kinetic analysis, the authors observed an unexpected behavior during light on/off experiments using a LED-NMR setup (Figure 19, A). When the light source was switched off, the reaction did not stop immediately, but the rate of product formation significantly decreased. Subsequently, experiments using a catalyst with ^{13}C-enriched CO ligands and LED-^{13}C-NMR monitoring were carried out to study if the light-mediated CO decomplexation that initiates catalysis is reversible. These monitoring experiments showed a decrease of dissolved ^{13}CO and a simultaneous increase of Fe-bound ^{13}CO upon switching off the light source (Figure 19, B). Constant illumination, on the contrary, results quickly in a steady state of both species that lasts until the substrate is fully consumed (Figure 19, C). This is indicative for an equilibrium between the catalytically inactive pre-catalyst **27** and the active Fe species **28** that can be externally controlled by light (Figure 19, D). It is important to note that the authors also found that removal of CO from the reaction mixture by sparging leads to catalyst deactivation, presumably due to the loss of another CO molecule from **27**. As

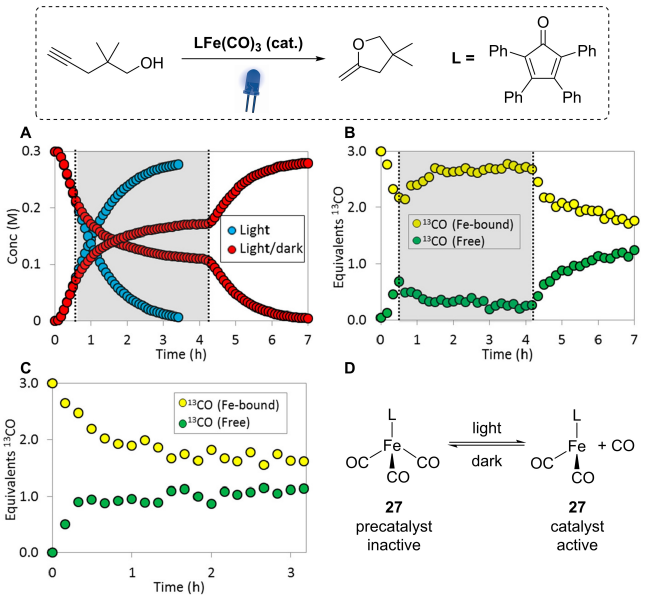

Figure 19. Reaction monitoring of a light induced cycloisomerization. The reaction proceeds quickly in presence of constant irradiation (blue) and does not stop when light is switched off (red) (A). LED-^{13}C-NMR shows light-mediated CO complexation in the dark (B) that does not occur upon constant irradiation (C) indicating that light mediated catalyst activation is reversible (D). Reproduced from ref. [59] with permission from the American Chemical Society.

© 2023 The Authors. ChemCatChem published by Wiley-VCH GmbH

such, best results were obtained using constant irradiation and a closed system with minimal headspace.

4. Conclusion

Reaction monitoring is slowly evolving as a valuable technique to acquire a better understanding of photocatalytic reactions. As shown in this minireview, such approaches are powerful tools that allow identifying reactive intermediates and access detailed kinetic information when combined with visual kinetic analysis. In addition, other aspects of photocatalytic reactions can be easily visualized. Together with other experiments, reaction monitoring paves the way towards a detailed mechanistic understanding of complex photocatalytic reactions. However, the field is still in its infancy and such methods are only rarely used, especially when compared to the plethora of new photocatalytic methodologies that appear in the literature on a daily basis.

To choose a suitable method, the type of mechanistic information required and the nature of the photochemical reaction of interest needs to be considered. Photoflow ESI-MS approaches allow qualitative analysis of intermediates, including short lived open-shell species. LED-NMR setups can also be used to track intermediates and additionally offer the opportunity for kinetic analysis. The small scale of LED-NMR experiments is characterized by short photon-path lengths, which facilitates photochemical experiments. Similarly, these dimensions ensure efficient heat-transfer and are ideally suited for investigating temperature effects in photocatalytic reactions. However, in case of multiphasic reactions, such as heterogeneous photocatalysis and reactions involving solid or gaseous reagents, efficient mixing is required to enable reliable and reproducible kinetic analysis. In such cases, FTIR probes are the technology of choice. This technique allows to run photocatalytic reactions under synthetically relevant conditions and is generally applicable for obtaining kinetic data, but does only provide limited structural information of intermediates and side-products. These individual limitations can be potentially addressed through combining two (or more) monitoring techniques. The combination of vibrational and optical spectroscopy probes is technically most straightforward.[25e] Moreover, fiber optic LED-NMR was combined with optical spectroscopy to simultaneously acquire UV/Vis and NMR spectra to monitor and quantify paramagnetic and diamagnetic species simultaneously in a time-resolved manner.[21] Combining ESI-MS with other monitoring techniques in a single device was, to the best of our knowledge, not yet realized for photocatalytic reactions. We anticipate that future efforts will overcome technical hurdles associated with combining multiple monitoring techniques to streamline mechanistic analysis of light-mediated transformations.

Acknowledgements

We gratefully acknowledge the Max Planck Society for 5generous financial support. A.M. and B.P. acknowledge the Deutsche Forschungsgemeinschaft (DFG, German Research Foundation) under Germany's Excellence Strategy-EXC 2008/1 (UniSysCat) – 390540038 for financial support. B.P. thanks the Boehringer Ingelheim Foundation for funding through the Plus 3 Perspectives Programme. Open Access funding enabled and organized by Projekt DEAL.

Conflict of Interest

The authors declare no conflict of interest.

Keywords: photocatalysis · reaction monitoring · mechanistic studies · kinetic analysis · reactive intermediates

[1] L. Marzo, S. K. Pagire, O. Reiser, B. König, *Angew. Chem. Int. Ed.* **2018**, *57*, 10034–10072; *Angew. Chem.* **2018**, *130*, 10188–10228.
[2] D. M. Arias-Rotondo, J. K. McCusker, *Chem. Soc. Rev.* **2016**, *45*, 5803–5820.
[3] A. Vega-Penaloza, J. Mateos, X. Companyo, M. Escudero-Casao, L. Dell'Amico, *Angew. Chem. Int. Ed.* **2021**, *60*, 1082–1097; *Angew. Chem.* **2021**, *133*, 1096–1111.
[4] S. Gisbertz, B. Pieber, *ChemPhotoChem* **2020**, *4*, 456–475.
[5] M. H. Shaw, J. Twilton, D. W. MacMillan, *J. Org. Chem.* **2016**, *81*, 6898–6926.
[6] F. Strieth-Kalthoff, M. J. James, M. Teders, L. Pitzer, F. Glorius, *Chem. Soc. Rev.* **2018**, *47*, 7190–7202.
[7] L. Capaldo, D. Ravelli, *Eur. J. Org. Chem.* **2017**, *2017*, 2056–2071.
[8] F. Glaser, C. Kerzig, O. S. Wenger, *Angew. Chem. Int. Ed.* **2020**, *59*, 10266–10284; *Angew. Chem.* **2020**, *132*, 10350–10370.
[9] S. Reischauer, B. Pieber, *iScience* **2021**, *24*, 102209.
[10] a) I. Ghosh, R. S. Shaikh, B. Konig, *Angew. Chem. Int. Ed.* **2017**, *56*, 8544–8549; *Angew. Chem.* **2017**, *129*, 8664–8669; b) M. Marchini, G. Bergamini, P. G. Cozzi, P. Ceroni, V. Balzani, *Angew. Chem. Int. Ed.* **2017**, *56*, 12820–12821; *Angew. Chem.* **2017**, *129*, 12996–12997; c) I. Ghosh, J. I. Bardagi, B. Konig, *Angew. Chem. Int. Ed.* **2017**, *56*, 12822–12824; *Angew. Chem.* **2017**, *129*, 12998–13000.
[11] N. A. Till, L. Tian, Z. Dong, G. D. Scholes, D. W. C. MacMillan, *J. Am. Chem. Soc.* **2020**, *142*, 15830–15841.
[12] L. Buzzetti, G. E. M. Crisenza, P. Melchiorre, *Angew. Chem. Int. Ed.* **2019**, *58*, 3730–3747; *Angew. Chem.* **2019**, *131*, 3768–3786.
[13] a) C. D. T. Nielsen, J. Burés, *Chem. Sci.* **2019**, *10*, 348–353; b) J. Bures, *Angew. Chem. Int. Ed.* **2016**, *55*, 16084–16087; *Angew. Chem.* **2016**, *128*, 16318–16321; c) D. G. Blackmond, *J. Am. Chem. Soc.* **2015**, *137*, 10852–10866.
[14] M. Sezen-Edmonds, J. E. Tabora, B. M. Cohen, S. Zaretsky, E. M. Simmons, T. C. Sherwood, A. Ramirez, *Org. Process Res. Dev.* **2020**, *24*, 2128–2138.
[15] H. E. Bonfield, T. Knauber, F. Levesque, E. G. Moschetta, F. Susanne, L. J. Edwards, *Nat. Commun.* **2020**, *11*, 804.
[16] F. Susanne, D. S. Smith, A. Codina, *Org. Process Res. Dev.* **2012**, *16*, 61–64.
[17] A. J. Pell, G. Pintacuda, C. P. Grey, *Prog. Nucl. Magn. Reson. Spectrosc.* **2019**, *111*, 1–271.
[18] V. Termopoli, E. Torrisi, G. Famiglini, P. Palma, G. Zappia, A. Cappiello, G. W. Vandergrift, M. Zvekic, E. T. Krogh, C. G. Gill, *Anal. Chem.* **2019**, *91*, 11916–11922.
[19] E. E. Kwan, S. G. Huang, *Eur. J. Org. Chem.* **2008**, *2008*, 2671–2688.
[20] a) I. Kuprov, M. Goez, P. A. Abbott, P. J. Hore, *Rev. Sci. Instrum.* **2005**, *76*, 084103; b) T. Kühn, H. Schwalbe, *J. Am. Chem. Soc.* **2000**, *122*, 6169–6174; c) C. Feldmeier, H. Bartling, E. Riedle, R. M. Gschwind, *J. Magn. Reson.* **2013**, *232*, 39–44; d) Y. Ji, D. A. DiRocco, J. Kind, C. M. Thiele, R. M. Gschwind, M. Reibarkh, *ChemPhotoChem* **2019**, *3*, 984–992; e) P.

© 2023 The Authors. ChemCatChem published by Wiley-VCH GmbH

Nitschke, N. Lokesh, R. M. Gschwind, *Prog. Nucl. Magn. Reson. Spectrosc.* **2019**, *114–115*, 86–134.
[21] L. K. G. Ackerman, J. I. Martinez Alvarado, A. G. Doyle, *J. Am. Chem. Soc.* **2018**, *140*, 14059–14063.
[22] J. E. Bramham, A. P. Golovanov, *Commun. Chem.* **2022**, *5*, 90.
[23] T. Paululat, M. Rabe, D. V. Berdnikova, *J. Magn. Reson.* **2021**, *327*, 106990.
[24] A. Mills, C. O'Rourke, *J. Org. Chem.* **2015**, *80*, 10342–10345.
[25] a) J. A. Malik, A. Madani, B. Pieber, P. H. Seeberger, *J. Am. Chem. Soc.* **2020**, *142*, 11042–11049; b) H. Pataki, I. Csontos, Z. K. Nagy, B. Vajna, M. Molnar, L. Katona, G. Marosi, *Org. Process Res. Dev.* **2013**, *17*, 493–499; c) W. Yang, A. S. Mondol, C. Stiebing, L. Marcu, J. Popp, I. W. Schie, *J. Biophotonics* **2019**, *12*, e201800447; d) I. Csontos, H. Pataki, A. Farkas, H. Bata, B. Vajna, Z. K. Nagy, G. Keglevich, G. J. Marosi, *Org. Process Res. Dev.* **2015**, *19*, 189–195; e) M. Rößler, P. U. Huth, M. A. Liauw, *React. Chem. Eng.* **2020**, *5*, 1992–2002; f) G. Amberchan, A. L. Allen, J. H. Golden, B. Singaram, J. Z. Zhang, *ACS Sustainable Chem. Eng.* **2021**, *9*, 6068–6078.
[26] J. M. Dreimann, E. Kohls, H. F. W. Warmeling, M. Stein, L. F. Guo, M. Garland, T. N. Dinh, A. J. Vorholt, *ACS Catal.* **2019**, *9*, 4308–4319.
[27] A. M. Tsedilin, A. N. Fakhrutdinov, D. B. Eremin, S. S. Zalesskiy, A. O. Chizhov, N. G. Kolotyrkina, V. P. Ananikov, *Mendeleev Commun.* **2015**, *25*, 454–456.
[28] Z. Han, X. Gu, S. Wang, L. Liu, Y. Wang, Z. Zhao, Z. Yu, *Analyst* **2020**, *145*, 3313–3319.
[29] C. F. Carter, H. Lange, S. V. Ley, I. R. Baxendale, B. Wittkamp, J. G. Goode, N. L. Gaunt, *Org. Process Res. Dev.* **2010**, *14*, 393–404.
[30] a) S. Schwolow, F. Braun, M. Rädle, N. Kockmann, T. Röder, *Org. Process Res. Dev.* **2015**, *19*, 1286–1292; b) T. A. Hamlin, N. E. Leadbeater, *Beilstein J. Org. Chem.* **2013**, *9*, 1843–1852.
[31] a) H. Lu, M. A. Schmidt, K. F. Jensen, *Lab Chip* **2001**, *1*, 22–28; b) J. Yue, F. H. Falke, J. C. Schouten, T. A. Nijhuis, *Lab Chip* **2013**, *13*, 4855–4863; c) F. Benito-Lopez, W. Verboom, M. Kakuta, J. G. E. Gardeniers, R. J. M. Egberink, E. R. Oosterbroek, A. van den Berg, D. N. Reinhoudt, *Chem. Commun.* **2005**, 2857–2859.
[32] a) M. V. Gomez, A. de la Hoz, *Beilstein J. Org. Chem.* **2017**, *13*, 285–300; b) P. Giraudeau, F.-X. Felpin, *React. Chem. Eng.* **2018**, *3*, 399–413.
[33] D. L. Browne, S. Wright, B. J. Deadman, S. Dunnage, I. R. Baxendale, R. M. Turner, S. V. Ley, *Rapid Commun. Mass Spectrom.* **2012**, *26*, 1999–2010.
[34] a) M. B. Plutschack, B. Pieber, K. Gilmore, P. H. Seeberger, *Chem. Rev.* **2017**, *117*, 11796–11893; b) M. Rodriguez-Zubiri, F.-X. Felpin, *Org. Process Res. Dev.* **2022**, *26*, 1766–1793; c) G. A. Price, D. Mallik, M. G. Organ, *J. Flow Chem.* **2017**, *7*, 82–86; d) C. N. Talicska, E. C. O'Connell, H. W. Ward, A. R. Diaz, M. A. Hardink, D. A. Foley, D. Connolly, K. P. Girard, T. Ljubicic, *React. Chem. Eng.* **2022**, *7*, 1419–1428.
[35] a) C. Cavedon, S. Gisbertz, S. Reischauer, S. Vogl, E. Sperlich, J. H. Burke, R. F. Wallick, S. Schrottke, W.-H. Hsu, L. Anghileri, Y. Pfeifer, N. Richter, C. Teutloff, H. Müller-Werkmeister, D. Cambié, P. H. Seeberger, J. Vura-Weis, R. M. van der Veen, A. Thomas, B. Pieber, *Angew. Chem. Int. Ed.* **2022**, *61*, e202211433; b) W.-H. Hsu, S. Reischauer, P. H. Seeberger, B. Pieber, D. Cambié, *Beilstein J. Org. Chem.* **2022**, *18*, 1123–1130.
[36] C. J. Taylor, J. A. Manson, G. Clemens, B. A. Taylor, T. W. Chamberlain, R. A. Bourne, *React. Chem. Eng.* **2022**, *7*, 1037–1046.
[37] a) W. Ding, K. A. Johnson, C. Kutal, I. J. Amster, *Anal. Chem.* **2003**, *75*, 4624–4630; b) W. Ding, K. A. Johnson, I. J. Amster, C. Kutal, *Inorg. Chem.* **2001**, *40*, 6865–6866; c) S. Chen, Q. Wan, A. K. Badu-Tawiah, *Angew. Chem. Int. Ed.* **2016**, *55*, 9345–9349; *Angew. Chem.* **2016**, *128*, 9491–9495; d) J. Zelenka, J. Roithová, *ChemBioChem* **2020**, *21*, 2232–2240; e) J. V. Burykina, V. P. Ananikov, *ChemPhotoChem* **2022**, *7*, *e202200175*.
[38] C. Feldmeier, H. Bartling, K. Magerl, R. M. Gschwind, *Angew. Chem. Int. Ed.* **2015**, *54*, 1347–1351; *Angew. Chem.* **2015**, *127*, 1363–1367.
[39] M. Goez, *Concepts Magn. Reson.* **1995**, *7*, 69–86.
[40] J. Zelenka, R. Cibulka, J. Roithová, *Angew. Chem. Int. Ed.* **2019**, *58*, 15412–15420; *Angew. Chem.* **2019**, *131*, 15558–15566.
[41] a) L. Shi, W. Xia, *Chem. Soc. Rev.* **2012**, *41*, 7687–7697; b) J. Hu, J. Wang, T. H. Nguyen, N. Zheng, *Beilstein J. Org. Chem.* **2013**, *9*, 1977–2001; c) J. W. Beatty, C. R. J. Stephenson, *Acc. Chem. Res.* **2015**, *48*, 1474–1484.
[42] A. G. Condie, J. C. González-Gómez, C. R. J. Stephenson, *J. Am. Chem. Soc.* **2010**, *132*, 1464–1465.
[43] H. Bartling, A. Eisenhofer, B. König, R. M. Gschwind, *J. Am. Chem. Soc.* **2016**, *138*, 11860–11871.
[44] Y. Cai, J. Wang, Y. Zhang, Z. Li, D. Hu, N. Zheng, H. Chen, *J. Am. Chem. Soc.* **2017**, *139*, 12259–12266.
[45] J. V. Burykina, N. S. Shlapakov, E. G. Gordeev, B. König, V. P. Ananikov, *Chem. Sci.* **2020**, *11*, 10061–10070.
[46] J. V. Burykina, A. D. Kobelev, N. S. Shlapakov, A. Y. Kostyukovich, A. N. Fakhrutdinov, B. König, V. P. Ananikov, *Angew. Chem. Int. Ed.* **2022**, *61*, e202116888.
[47] W. Ai, Q. Yang, Y. Gao, X. Liu, H. Liu, Y. Bai, *Anal. Chem.* **2020**, *92*, 11967–11972.
[48] D. M. Schultz, F. Lévesque, D. A. DiRocco, M. Reibarkh, Y. Ji, L. A. Joyce, J. F. Dropinski, H. Sheng, B. D. Sherry, I. W. Davies, *Angew. Chem. Int. Ed.* **2017**, *56*, 15274–15278; *Angew. Chem.* **2017**, *129*, 15476–15480.
[49] K. Chen, N. Berg, R. Gschwind, B. König, *J. Am. Chem. Soc.* **2017**, *139*, 18444–18447.
[50] U. Lennert, P. B. Arockiam, V. Streitferdt, D. J. Scott, C. Rödl, R. M. Gschwind, R. Wolf, *Nat. Catal.* **2019**, *2*, 1101–1106.
[51] R. Rothfelder, V. Streitferdt, U. Lennert, J. Cammarata, D. J. Scott, K. Zeitler, R. M. Gschwind, R. Wolf, *Angew. Chem. Int. Ed.* **2021**, *60*, 24650–24658; *Angew. Chem.* **2021**, *133*, 24855–24863.
[52] K. L. Skubi, W. B. Swords, H. Hofstetter, T. P. Yoon, *ChemPhotoChem* **2020**, *4*, 685–690.
[53] W. B. Swords, S. J. Chapman, H. Hofstetter, A. L. Dunn, T. P. Yoon, *J. Org. Chem.* **2022**, *87*, 11776–11782.
[54] J. Zheng, W. B. Swords, H. Jung, K. L. Skubi, J. B. Kidd, G. J. Meyer, M.-H. Baik, T. P. Yoon, *J. Am. Chem. Soc.* **2019**, *141*, 13625–13634.
[55] S. Gisbertz, S. Reischauer, B. Pieber, *Nat. Catal.* **2020**, *3*, 611–620.
[56] Y. Ben-Tal, G. C. Lloyd-Jones, *J. Am. Chem. Soc.* **2022**, *144*, 15372–15382.
[57] C. Cavedon, E. T. Sletten, A. Madani, O. Niemeyer, P. H. Seeberger, B. Pieber, *Org. Lett.* **2021**, *23*, 514–518.
[58] M. A. Cismesia, T. P. Yoon, *Chem. Sci.* **2015**, *6*, 5426–5434.
[59] D. Lehnherr, Y. Ji, A. J. Neel, R. D. Cohen, A. P. J. Brunskill, J. Yang, M. Reibarkh, *J. Am. Chem. Soc.* **2018**, *140*, 13843–13853.

Manuscript received: December 12, 2022
Revised manuscript received: February 23, 2023
Accepted manuscript online: February 27, 2023
Version of record online: March 24, 2023

© 2023 The Authors. ChemCatChem published by Wiley-VCH GmbH